

# Aberrant iron accumulation and oxidized status of erythroid-specific $\delta$ -aminolevulinate synthase (ALAS2)-deficient definitive erythroblasts

Hideo Harigae, Osamu Nakajima, Naruyoshi Suwabe, Hisayuki Yokoyama, Kazumichi Furuyama, Takeshi Sasaki, Mitsuo Kaku, Masayuki Yamamoto, and Shigeru Sassa

*Alas2* encodes the erythroid-specific  $\delta$ -aminolevulinate synthase (ALAS2 or ALAS-E), the first enzyme in heme biosynthesis in erythroid cells. Mice with the *Alas2*-null phenotype showed massive cytoplasmic, but not mitochondrial, iron accumulation in their primitive erythroblasts. Because these animals died by day 11.5 in utero, studies of iron metabolism in definitive erythroblasts were not possible using the in vivo model. In this study, embryonic stem (ES) cells lacking the *Alas2* gene were induced to undergo differentiation to the definitive erythroblast stage in culture, and the phenotype of *Alas2*-null definitive erythroblasts was

examined. *Alas2*-null definitive erythroblasts cell pellets were entirely colorless due to a marked deficiency of heme, although their cell morphology was similar to that of the wild-type erythroblasts. The level of expression of erythroid-specific genes in *Alas2*-null definitive erythroblasts was also similar to that of the wild-type erythroblasts. These findings indicate that *Alas2*-null definitive erythroblasts developed to a stage similar to that of the wild-type erythroblasts, which were also shown to be very similar to the bone marrow erythroblasts in vivo. In contrast, *Alas2*-null definitive erythroblasts contained 15 times more nonheme

iron than did the wild-type erythroblasts, and electron microscopy found this iron to be distributed in the cytoplasm but not in mitochondria. Consistent with the aberrant increase in iron, *Alas2*-null definitive erythroblasts were more peroxidized than wild-type erythroblasts. These findings suggest that ALAS2 deficiency itself does not interfere with the development of definitive erythroid cells, but it results in a profound iron accumulation and a peroxidized state in erythroblasts. (Blood. 2003; 101:1188-1193)

© 2003 by The American Society of Hematology

## Introduction

Heme, the prosthetic group of hemoproteins, is essential for the function of all aerobic cells. Approximately 85% of heme in the body is synthesized by erythroid cells and utilized for hemoglobin formation.<sup>1</sup> Besides its main function as an oxygen carrier in the hemoglobin molecule, heme also plays an important role in erythroid cellular development, and its deficiency has been associated with dysregulation of protein synthesis,<sup>2</sup> apoptosis of cells,<sup>3</sup> and X-linked sideroblastic anemia (XLSA).<sup>4-7</sup>

The erythroid-specific  $\delta$ -aminolevulinate synthase, ALAS2 (or ALAS-E), is the first enzyme in the heme biosynthetic pathway and is exclusively expressed in erythroid cells.<sup>8,9</sup> In human beings, various mutations of the *ALAS2* gene, which is located at Xp11.21, have been reported in patients with XLSA, an X chromosome-linked hypochromic and microcytic anemia characterized by the presence of ring sideroblasts in bone marrow.<sup>4-7</sup> It is thought that ALAS2 deficiency in patients with XLSA results in a decreased supply of protoporphyrin IX, which in turn causes an excessive accumulation of iron in erythroblasts, ultimately resulting in the formation of ring sideroblasts. Such an iron overload is likely to disturb cellular reduction-oxidation state and may result in the shortening of the cellular lifetime. These findings point to the

critical role of ALAS2 in the cellular differentiation and survival of erythroid cells. In our previous in vivo study of mice with ALAS2 deficiency, we found a maturation arrest and a massive iron accumulation in *Alas2*-null primitive erythroid cells.<sup>10</sup> This iron accumulation was observed exclusively in the cytoplasm, and not in mitochondria, which is the typical site of iron accumulation in patients with XLSA. These mice died by day 11.5 in utero; therefore, studies on iron metabolism in erythroblasts at a later stage, such as definitive erythroblasts, were not possible, and it remained unclear whether the absence of sideroblasts in mice was due to the fact that only the primitive erythroblasts were examined<sup>10</sup> or other reasons.

In this study, we prepared *Alas2*-null definitive erythroblasts from *Alas2*-null embryonic stem (ES) cells in culture and compared their characteristics with those of the wild-type definitive erythroblasts and of mature bone marrow erythroblasts isolated from mice. Our results demonstrate that ALAS2 deficiency leads to excessive iron accumulation in the cytoplasm of definitive erythroblasts, similar to the finding in *Alas2*-null primitive erythroblasts.<sup>10</sup> These findings are, however, in contrast to the mitochondrial iron accumulation seen in bone marrow erythroblasts of patients with XLSA.

From the Departments of Molecular Diagnostics, Rheumatology and Hematology, and Molecular Biology, Tohoku University School of Medicine, Sendai, Japan; Center for Tsukuba Advanced Research Alliance, University of Tsukuba, Japan, and Rockefeller University, New York, NY.

Submitted December 27, 2001; accepted August 30, 2002. Prepublished online as *Blood* First Edition Paper, October 3, 2002; DOI 10.1182/blood-2002-01-0309.

Supported in part by Grant-in-Aid from the Ministry of Education, Science and

Culture of Japan (H.H.) and by NIH NIDDK grant DK 32890 (S.S.).

**Reprints:** Hideo Harigae, Department of Molecular Diagnostics, Tohoku University School of Medicine, 1-1 Seiryomachi, Aoba-ku, Sendai 980-8574, Japan; e-mail: harigae@mail.cc.tohoku.ac.jp.

The publication costs of this article were defrayed in part by page charge payment. Therefore, and solely to indicate this fact, this article is hereby marked "advertisement" in accordance with 18 U.S.C. section 1734.

© 2003 by The American Society of Hematology

## Materials and methods

### Cell culture, sorting, and transmission electron microscopy

*Alas2*-null ES cells<sup>10</sup> and the wild-type ES cells were cultivated with OP9, a macrophage colony-stimulating factor (M-CSF)-deficient mouse stromal cell line, and were induced to undergo erythroid differentiation as described previously, with only minor modifications.<sup>11</sup> Namely, ES cells were plated onto confluent OP9 cells at a concentration of  $5 \times 10^3$  cells per well in a 6-well plate using minimum essential medium alpha medium ( $\alpha$ -MEM; Gibco BRL, Grand Island, NY) supplemented with 20  $\mu$ M  $\beta$ -mercaptoethanol, 2 U/mL human erythropoietin, 50 ng/mL murine stem cell factor (SCF) (Gibco Lifetec Oriental, Rockville, MD), and 10 ng/mL vascular endothelial growth factor (VEGF) (Peprotech, Rocky Hill, NJ). Human erythropoietin was kindly provided by Chugai Pharmaceutical, Tokyo, Japan. On day 3 of culture, one half volume of the culture media was replenished with fresh medium, and incubation was continued to day 5 when total cells were harvested by trypsinization. They were transferred to a P100 culture dish, which had been covered with confluent OP9 cells, and incubated in the same culture media but without VEGF. Primitive erythroblasts were collected by harvesting all floating cells by centrifugation on day 8. To collect definitive erythroblasts, total cells collected on day 10 by pipetting were transferred to a new OP9 cell-plated culture dish, and then the incubation was continued to day 14 when all floating cells were collected. TER119<sup>+</sup> bone marrow erythroid cells were isolated from the normal mouse bone marrow and sorted by using a magnetic cell sorting system (MACS; Miltenyi Biotec, Gladbach, Germany). Transmission electron microscopy (TEM) was performed using H-7600 Transmission Electron Scope (Horiba, Kyoto, Japan) as described previously.<sup>10</sup>

### Reverse-transcriptase polymerase chain reaction (RT-PCR)

Total RNA was extracted from cells by the guanidine-phenol method.<sup>12</sup> Complementary DNA was synthesized from 2  $\mu$ g total RNA in 20  $\mu$ L of the reaction mixture containing 0.5  $\mu$ g oligo(dT)<sub>12-18</sub>, 200 units of Moloney murine leukemia virus reverse transcriptase (SuperscriptTMII, Gibco, Gaithersburg, MD), 20 mM Tris (tris(hydroxymethyl)aminomethane) HCl (pH 9.4), 50 mM KCl, 2.5 mM MgCl<sub>2</sub>, 0.5 mM of each deoxyribonucleoside triphosphate (dNTP), and 10 mM dithiothreitol (DTT). Target genes were then amplified by PCR with a set of specific primers using 1  $\mu$ L cDNA solution as a template. PCR was performed using an appropriate number of cycles for amplification where the linearity had been verified. Durations for denaturation, annealing, and extension were 1 minute each except for ALAS1, for which 20 seconds, 5 seconds, and 1 minute were used for those processes, respectively. Temperature for denaturation and extension were 94°C and 72°C, respectively, for all PCRs. Temperature for annealing was 60°C for ALAS1 and  $\beta$ -actin and 56°C for other genes. Sequences of each primer used are as follows: ALAS1 sense: 5'-CATCTTACCACCTCCTTGCCACCA, antisense: 5'-CTATGTGGGTATGGTAATGGCCTGGG; ALAS2 sense: 5'-GATCCAAGGCATTCGCAACA, antisense: 5'-GATGGCCTGCACATAGATGC;  $\beta$ -actin sense: 5'-GTGACGAGGCCAGAGCAAG, antisense: 5'-AGGGGCCGACTCATCGTAC;  $\beta$ -major globin sense: 5'-ATGGTGCACCTGACTGATGCTG, antisense: 5'-GGTTTAGTGGTACTTGTGAGCC; DMT1 sense: 5'-GGTCTGACATGCAGGAAGT, antisense: 5'-CAAAGACATTGATGATGAAAG;  $\epsilon$ y globin sense: 5'-AACCTCATCAATGGCCTGTGG, antisense: 5'-TCAGTGGTACTTGTGGACAGC; GATA-1 sense: 5'-ACTCGTCATACCACTAAGGT, antisense: 5'-AGTGTCTGTAGGCCTCAGCT; HO-1 sense: 5'-ACGCATATACCCGCTACCTG, antisense: 5'-AAGCTGAGAGTGAGGACCCA; NF-E2 sense: 5'-AACTTGCCGGTAGATGACTTTAAT, antisense: 5'-CACCAAATACTCCAGGTGATATG.

### Flow cytometric analysis

Floating cells collected on day 8 and day 14 were incubated with TER119 (Pharmingen, San Diego, CA), an antibody against the mature erythroid-specific antigen,<sup>13</sup> and anti-CD71, an antibody for transferrin receptor (Caltag, Burlingame, CA). For apoptosis analysis, floating cells harvested

on day 14 were incubated with annexin V and propidium iodide (PI), according to the manufacturer's protocol (MBL, Nagoya, Japan). Flow cytometric analysis was performed using FACSCalibur (Becton Dickinson, Lincoln Park, NJ).

### Heme assay

Heme content was determined fluorometrically using  $10^5$  cells per assay as described previously.<sup>14</sup> All determinations were made in triplicates, and heme contents were expressed as picomoles per  $10^6$  cells.

### Iron content

Cells were dissolved in nitric acid, and iron content in the solution was determined by atomic absorption spectrometry using Z-5010 type polarized Zeeman Atomic Absorption Spectrometer (Hitachi High Technology, Hitachinaka, Japan).<sup>10</sup>

### Measurement of intracellular reactive oxygen intermediates

Redox state of cells was determined as described previously<sup>15</sup> but in the absence of H<sub>2</sub>O<sub>2</sub> in the assay mixture. 2',7-dichlorodihydrofluorescein (DCFHDA, Sigma, St Louis, MO) was used as a fluorogenic substrate for an oxidation reaction with cells. The intensity of fluorescence corresponds to the amount of cellular peroxidized substances. Bone marrow cells and floating cells harvested on day 14 from culture were washed in phosphate-buffered saline (PBS) and first reacted with phycoerythrin (PE)-conjugated TER119 for 15 minutes. After washing with PBS, cells were incubated with 10  $\mu$ M DCFHDA in PBS containing 2% fetal bovine serum (FBS) for 30 minutes at room temperature. Fluorescence generated by the cellular oxidation of DCFHDA was determined by flow cytometry.

### Immunostaining

Immunostaining for hemoglobin was performed as described previously.<sup>16</sup> Briefly, floating cells harvested on day 8 and day 14 were centrifuged using Cytospin 3 (Shandon, Pittsburgh, PA). After fixation in acetone-methanol, cells were incubated with rabbit antimouse  $\beta$ -major globin antibody (Research Plus, Bayonne, NJ) or rabbit antimouse  $\epsilon$ y globin antibody<sup>17</sup> at 4°C for overnight and then incubated with horseradish peroxidase (HRP)-conjugated goat antirabbit antibody at 4°C for 6 hours. Positive signals were visualized by incubation with diaminobenzidine (DAB).

## Results

### Morphology of *Alas2*-null erythroblasts

The type of globin expressed in erythroblasts collected on day 8 and day 14 was examined by immunostaining. It was found that  $\beta$ -major globin, an adult globin, was expressed in erythroblasts harvested on day 14 (Figure 1D), while  $\epsilon$ y globin, an embryonic globin, was expressed in erythroblasts harvested on day 8 (Figure 1A). Conversely,  $\beta$ -major globin was not detected in erythroblasts harvested on day 8 (Figure 1B), while  $\epsilon$ y globin was not detected in erythroblasts harvested on day 14 (Figure 1C). These findings indicate that the erythroblasts harvested on day 8 and on day 14 indeed correspond to primitive and definitive erythroblasts, respectively.

Morphologic examination of these cells was performed using May-Grünwald Giemsa stain. The wild-type (Figure 2A) and *Alas2*-null primitive erythroblasts (Figure 2B) were both significantly larger and more basophilic than their corresponding definitive erythroblasts collected on day 14 (Figure 2C and D, respectively). Both *Alas2*-null and the wild-type definitive erythroblasts were also smaller than normal proerythroblasts in the bone marrow in size, contained denser chromatin (data not shown), and were thus

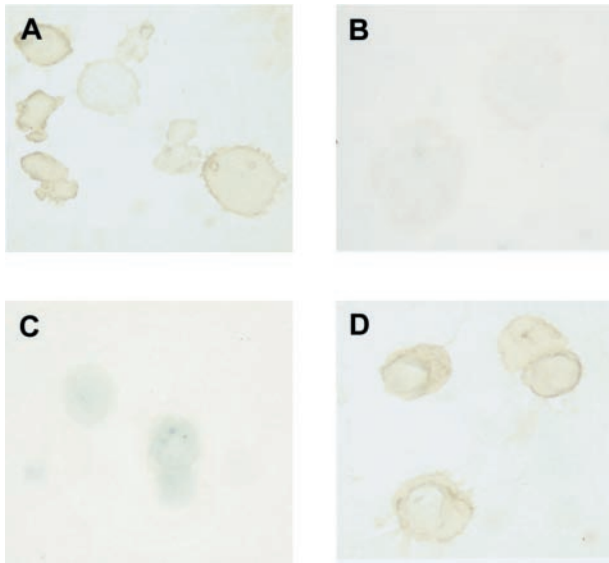


**Figure 1. Expression of embryonic and adult globin in erythroblasts derived from ES cells in vitro.** Immunostaining of  $\epsilon\gamma$  and  $\beta$ -major globin was described in "Materials and methods." (A) Incubation of day 8 erythroblasts with rabbit antimouse  $\epsilon\gamma$  globin. (B) Incubation of day 8 erythroblasts with rabbit antimouse  $\beta$ -major globin. (C) Incubation of day 14 erythroblasts with rabbit antimouse  $\epsilon\gamma$  globin. (D) Incubation of day 14 erythroblasts with rabbit antimouse  $\beta$ -major globin. Original magnification  $\times 1000$ .

considered to correspond to polychromatophilic or orthochromatophilic erythroblasts. While the morphology of *Alas2*-null definitive erythroblasts was similar to that of the wild-type definitive erythroblasts, the cell pellet collected from *Alas2*-null erythroblasts was entirely colorless (the right tube in Figure 2E).

Heme content in these cells, determined by fluorometry, was  $1620 \pm 45$  pmol/ $10^6$  cells and  $120 \pm 15$  pmol/ $10^6$  cells for the wild-type and *Alas2*-null definitive erythroblasts, respectively ( $P < .001$ ,  $n = 3$ ). Interestingly, the heme content of the wild-type erythroblasts collected from culture was only slightly less than that of TER119<sup>+</sup> erythroid cells isolated from normal mouse bone marrow ( $2430 \pm 114$  pmol/ $10^6$  cells), indicating that the wild-type definitive erythroblasts differentiated to a stage very close to the mature erythroblasts in the bone marrow.

Next, iron content was determined by atomic absorption spectrometry. In contrast to heme content, *Alas2*-null definitive erythroblasts contained a significantly larger amount of iron ( $6946 \pm 200$  pmol/ $10^6$  cells,  $n = 3$ ) than the wild-type definitive erythroblasts cells ( $2053 \pm 200$  pmol/ $10^6$  cells,  $n = 3$ ) ( $P < .001$ ). Thus, the nonheme iron amounts, calculated on the basis of total iron and heme content, were 433 pmol/ $10^6$  cells and 6826 pmol/ $10^6$  cells for the wild-type and *Alas2*-null erythroblasts, respectively. Hence, the nonheme iron content in *Alas2*-null erythroblasts was nearly 16-fold that of wild-type erythroblasts and accounted for most of the total iron content in the cell. Total and nonheme iron content in TER119<sup>+</sup> bone marrow erythroid cells was 3210 pmol/ $10^6$  cells and 780 pmol/ $10^6$  cells, respectively. These findings indicate that *Alas2*-null definitive erythroblasts had accumulated an excessive amount of nonheme iron in the cell and were markedly deficient in heme.

Conventional Prussian blue staining for iron did not detect an increase in iron in *Alas2*-null definitive erythroblasts (data not shown). When TEM, a more sensitive technique than the conventional iron staining, was used for examination of cellular iron, it was found that there was a diffuse accumulation of ferritin iron in the cytoplasm (Figure 3B), but not in mitochondria (Figure 3C), in

*Alas2*-null definitive erythroblasts, as compared with the wild-type definitive erythroblasts (Figure 3A).

#### Expression of erythroid-specific genes or genes involved in iron metabolism

Next, the level of expression of erythroid-specific genes was examined by RT-PCR. The  $\epsilon\gamma$  globin mRNA was virtually absent in TER119<sup>+</sup> erythroblasts from bone marrow and in *Alas2*-null definitive erythroblasts, while it was barely detected in the wild-type definitive erythroblasts (Figure 4A). Its level was, however, markedly lower than that in primitive erythroblasts (data not shown). Similar amounts of  $\beta$ -major globin mRNA were expressed both in *Alas2*-null and the wild-type definitive erythroblasts as well as in TER119<sup>+</sup> bone marrow erythroid cells (Figure 4A). The levels of GATA-1 and NF-E2 mRNA were similar for both *Alas2*-null and the wild-type definitive erythroblasts (Figure 4A) and comparable to GATA-1 and NF-E2 mRNA levels observed in TER119<sup>+</sup> bone marrow erythroid cells (Figure 4A), suggesting that both *Alas2*-null and the wild-type definitive erythroblasts had been fully differentiated to a stage comparable to mature bone marrow erythroblasts.

#### Heme and iron metabolism in *Alas2*-null definitive erythroblasts

In addition to the erythroid-specific genes, expression of genes involved in heme synthesis and iron metabolism was also examined. ALAS2 mRNA was expressed both in the wild-type definitive erythroblasts and in TER119<sup>+</sup> bone marrow erythroblasts, and their levels were very similar (Figure 4B). ALAS2 mRNA was not detectable in *Alas2*-null erythroblasts, reflecting the fact that exons

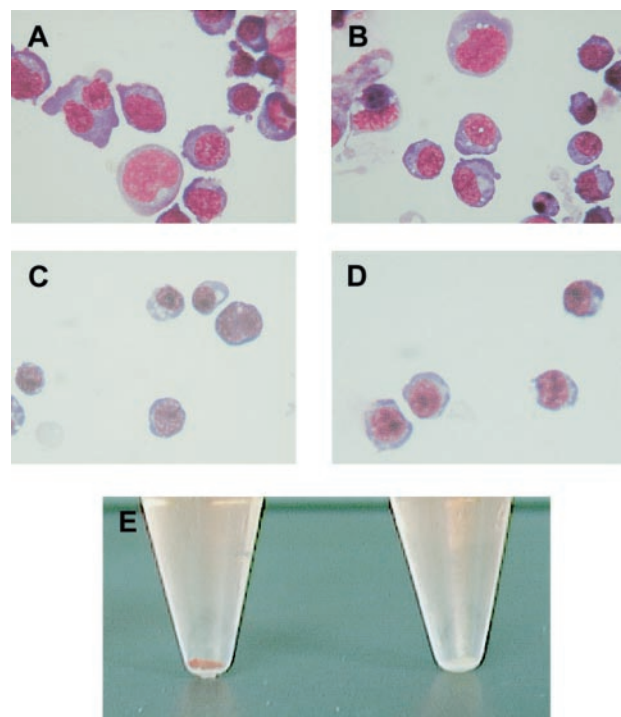
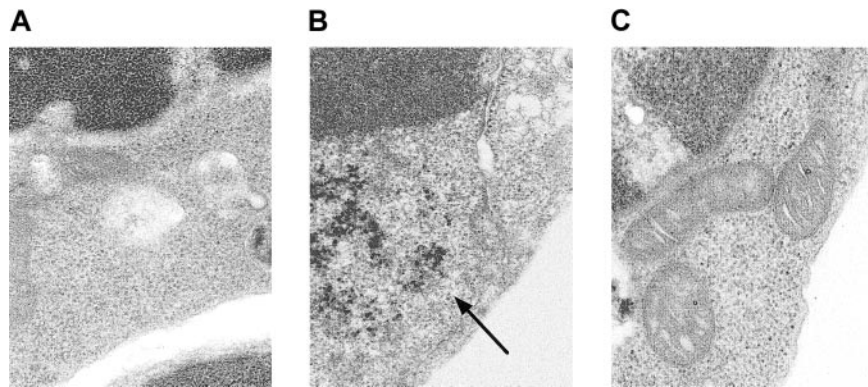


**Figure 2. Morphology of erythroblasts derived from ES cells in vitro.** The wild-type and *Alas2*-null ES cells were cultured on a feeder layer of OP9 cells, and floating cells on day 8 and day 14 were collected as primitive and definitive erythroblasts, respectively. (A) The wild-type primitive erythroblasts. (B) *Alas2*-null primitive erythroblasts. (C) The wild-type definitive erythroblasts. (D) *Alas2*-null definitive erythroblasts. Original magnification,  $\times 400$  for panels A-D. (E) Cell pellet of the wild-type (left, red) and *Alas2*-null (right, white) definitive erythroblasts.



**Figure 3. Electron microscopic analysis of *Alas2*-null definitive erythroblasts.** The wild-type and *Alas2*-null definitive erythroblasts were examined by TEM. (A) The wild-type definitive erythroblasts. (B) *Alas2*-null definitive erythroblasts (ferritin aggregates indicated by an arrow). (C) *Alas2*-null definitive erythroblasts (no iron granules in mitochondria). The original magnification was  $\times 50\ 000$  for all panels.



8 through 10 of the *Alas2* gene had been replaced by a neomycin-resistant cassette that abolished amplification, because primers anneal to exon 7 and exon 10 (Figure 4B).<sup>18</sup> Interestingly, ALAS1 mRNA was markedly increased in *Alas2*-null definitive erythroblasts, while the level was decreased in the wild-type definitive erythroblasts, compared with that in TER119<sup>+</sup> bone marrow erythroid cells (Figure 4B). An elevated expression of ALAS1 mRNA had also been observed in *Alas2*-null primitive erythroblasts (data not shown). In contrast, HO-1 mRNA, which encodes the rate-limiting enzyme in the heme catabolic pathway and is known to be inducible by heme, was markedly expressed in the wild-type definitive erythroblasts compared with *Alas2*-null definitive erythroblasts (Figure 4B), suggesting a heme-mediated induction of HO-1. The level of HO-1 mRNA in the wild-type definitive erythroblasts collected from culture was also higher than that in TER119<sup>+</sup> bone marrow erythroid cells. Because *HO-1* is a stress-responsive gene and is known to respond to various oxidative stimuli,<sup>19</sup> this finding may reflect a more highly oxidized condition in the erythroblasts that were collected from culture compared with those that were isolated from the bone marrow of normal mice. In contrast to the rate-limiting enzymes in heme synthesis and catabolism, the level of mRNA for DMT1, an iron transporter, was similar for both *Alas2*-null and the wild-type definitive erythroblasts (Figure 4B).

**Expression of TER119 and transferrin receptor in *Alas2*-null definitive erythroblasts**

By flow cytometry, TER119, a marker for erythroblasts that have differentiated to the erythroid colony-forming unit (CFU-E) stage and beyond CFU-E, was also found to be expressed in *Alas2*-null definitive erythroblasts (Figure 5D), at a level similar to that in the wild-type definitive erythroblasts (Figure 5C). This situation was quite different from that in primitive erythroblasts in that TER119 expression was suppressed in *Alas2*-null primitive erythroblasts (Figure 5B), as compared with the wild-type primitive erythroblasts (Figure 5A), but consistent with the findings in primitive erythroblasts from *Alas2*-targeted mice in vivo.<sup>10</sup> Similar to TER119 expression, transferrin receptor expression levels were similar between the wild-type and *Alas2*-null definitive erythroblasts (Figure 5C and D, respectively) and lower in *Alas2*-null primitive erythroblasts than in wild-type primitive erythroblasts (Figure 5B and A, respectively). These findings suggest that while ALAS2 deficiency results in a maturation arrest in primitive erythropoiesis, it does not interfere with the normal development of definitive erythropoiesis.

**Redox status of *Alas2*-null erythroblasts**

Because iron is known to facilitate peroxidation of lipids in the cell membrane,<sup>20</sup> *Alas2*-null definitive erythroblasts may be more oxidized than the wild-type definitive erythroblasts. We examined

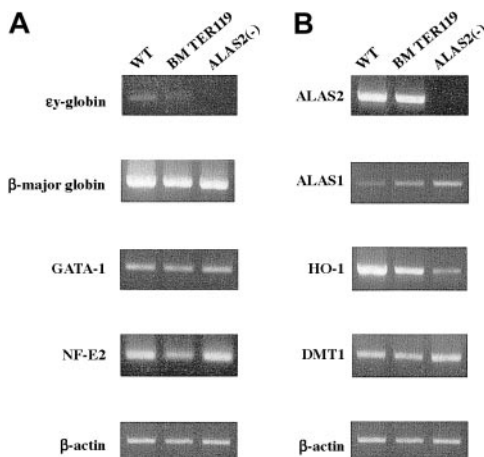


**Figure 4. Expression of erythroid-specific genes and genes involved in heme biosynthesis and catabolism.** Total RNA was extracted from the wild-type and *Alas2*-null definitive erythroblasts or TER119<sup>+</sup> bone marrow erythroid cells, and 2  $\mu$ g total RNA was reverse transcribed. Then, target genes were amplified by PCR with a set of specific primers using 1  $\mu$ L cDNA solution as a template. (A) Erythroid-specific genes. (B) Genes involved in heme biosynthesis, catabolism, and iron metabolism. Although the *Alas2* gene is both an erythroid-specific and a heme pathway gene, its expression is shown in panel B.

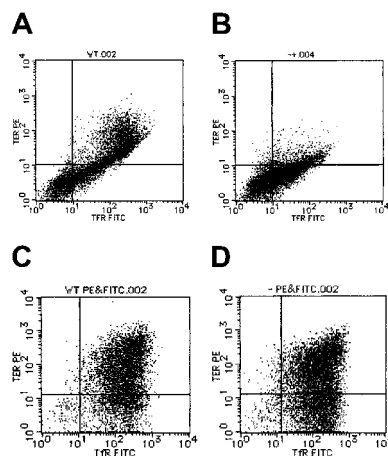


**Figure 5. Expression of TER119 and transferrin receptor in ES-derived erythroblasts.** Flow cytometry for TER119 and transferrin receptor expression was described in "Materials and methods." (A) The wild-type primitive erythroblasts. (B) *Alas2*-null primitive erythroblasts. (C) The wild-type definitive erythroblasts. (D) *Alas2*-null definitive erythroblasts. TER119 expression is shown on the ordinate (y-axis), while transferrin receptor expression is shown on the abscissa (x-axis).

the oxidation-reduction state of wild-type and *Alas2*-null definitive erythroblasts harvested on day 14, as well as TER119<sup>+</sup> bone marrow erythroid cells, using flow cytometry with DCFHDA as the fluorogenic substrate. As shown in Figure 6, the fluorescence intensity, indicating the oxidation of DCFHDA following incubation with cells, was higher in *Alas2*-null definitive erythroblasts than in wild-type definitive erythroblasts. The fluorescence intensity in TER119<sup>+</sup> bone marrow erythroid cells was much lower than in wild-type definitive erythroblasts (Figure 6C), suggesting that erythroblasts collected from culture are significantly more oxidized than mature erythroblasts isolated from bone marrow of live animals.

Finally, to study the effect of such an oxidized status on cell aging, an apoptosis assay was performed by flow cytometry using annexin V as a marker for apoptosis. A significant fraction of both *Alas2*-null and the wild-type definitive erythroblasts was found to be apoptotic, presumably reflecting the fact that they have completed cell differentiation, as indicated by their floating nature off from the OP9 feeder layer. This finding also suggests that both *Alas2*-null and the wild-type definitive erythroblasts collected on day 14 in culture were so peroxidized that they could not be differentiated from each other.

## Discussion

Various mutations of the *Alas2* gene have been reported in patients with XLSA and are thought to be responsible for the development of hypochromic anemia with ring sideroblasts. Most of these mutations were found in the catalytic domain of the ALAS2 protein and suggest that functional ALAS2 deficiency is responsible for the development of XLSA.<sup>4-7</sup> Our previous study in *Alas2*-targeted mice provided the experimental proof that ALAS2 deficiency in fact results in abnormal iron accumulation in primitive erythroblasts in vivo.<sup>10</sup> However, the iron accumulation in these cells was diffusely distributed in the cytoplasm<sup>10</sup> and was quite distinct from the mitochondrial iron accumulation, known as ring sideroblasts,

seen in patients with XLSA. Because *Alas2*-null mice died by embryonic day 11.5 before definitive erythropoiesis developed, it was not possible to examine the iron status in definitive erythroblasts.

To examine iron metabolism in definitive erythroblasts, we prepared *Alas2*-null definitive erythroblasts from ES cells using an in vitro differentiation system with OP9 stromal cells.<sup>11</sup> ES cells were allowed to differentiate to a stage comparable to definitive erythroblasts, as judged by morphologic and gene expression studies. Namely, the wild-type ES cells, which were differentiated to the erythroid lineage for 8 days and 14 days in culture, produced floating cells that corresponded to primitive and definitive erythroblasts, respectively, as judged by the presence of  $\epsilon$  and  $\beta$ -major hemoglobin (Figure 1A,D). *Alas2*-null definitive erythroblasts also differentiated to a stage similar to the wild-type cells, as judged by their similar morphology and similar expression of erythroid-specific genes (Figure 4A). In contrast, the color of cell pellets of *Alas2*-null definitive erythroblasts was white, suggesting a major lack of heme, while the color of cell pellets of the wild-type definitive erythroblasts was intensely red, indicating active hemoglobin synthesis (Figure 2E). This finding was confirmed by chemical quantification of cellular heme by fluorometry, which demonstrated that *Alas2*-null definitive erythroblasts contained less than 10% heme found in the wild-type definitive erythroblasts. Conversely, the total iron content of the *Alas2*-null definitive erythroblasts was more than 3-fold compared with that of wild-type erythroblasts. The increase in total iron content was largely accounted for by a marked increase in nonheme iron content that was about 16-fold higher in *Alas2*-null definitive erythroblasts than in the wild-type definitive erythroblasts. These findings clearly establish the fact that ALAS2 deficiency results in aberrant iron accumulation both in primitive<sup>10</sup> and definitive erythropoiesis.

An important difference in the findings between mice and human patients with XLSA should be noted. Namely, no ring sideroblasts were found in the mouse models of ALAS2 deficiency in culture, while ring sideroblasts are the cytologic hallmark of XLSA in human beings. The reason for the observed discrepancy remains unclear, but several possibilities can be speculated. First, mice with ALAS2 deficiency may not be as prone to form sideroblasts as do human patients with XLSA. However, this is unlikely because transient siderocyte formation with mitochondrial iron deposits has been reported in flexed-tail (*ff*) mice.<sup>21</sup> Secondly, the lack of sideroblasts in culture might reflect a limitation inherent in the tissue culture method that may not allow sideroblast formation. However, there have been occasional reports of successful sideroblast formation in culture from bone marrow cells of patients with primary acquired sideroblastic anemia.<sup>22,23</sup> Thirdly, the observed difference between *Alas2*-null definitive erythroblasts and sideroblasts in patients with XLSA might reflect incomplete differentiation of *Alas2*-null definitive erythroblasts. However, our study showed that *Alas2*-null definitive erythroblasts developed to a stage comparable to that of normal mature erythroblasts. Fourthly, the red-ox state in cultured cells may be significantly different from that of the normal erythroblasts in the bone marrow. In fact, our findings indicate that *Alas2*-null definitive erythroblasts are significantly more peroxidized than bone marrow erythroblasts, and this may restrict the development of sideroblasts. Lastly, other factors along with ALAS2 deficiency may be necessary for the development of sideroblasts. This is an intriguing possibility that is currently being explored by culturing definitive erythroblasts that express a low level of ALAS2 activity. Such cells should mimic the condition of the bone marrow erythroblasts in patients with XLSA better than *Alas2*-null erythroblasts.

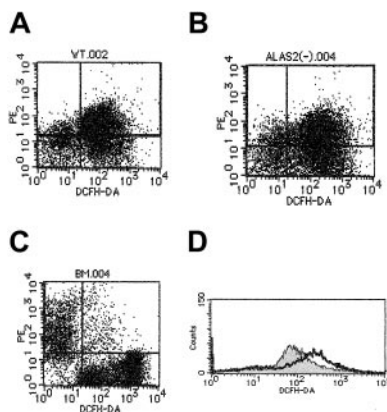


**Figure 6. Redox state analysis of definitive erythroblasts derived from ES cells.** Redox state of cells was assayed as described in "Materials and methods," using DCFHDA as a fluorogenic substrate, but in the absence of H<sub>2</sub>O<sub>2</sub>, and cellular fluorescence intensity was examined by flow cytometry. (A) The wild-type definitive erythroblasts. (B) *Alas2*-null definitive erythroblasts. (C) Mouse bone marrow cells. TER119 fluorescence is shown on the ordinate (y-axis), while DCFHDA-mediated fluorescence is shown on the abscissa (x-axis). Note in the bone marrow TER119<sup>+</sup> cells (C), cell population at the upper left exhibited a significantly lower level of DCFHDA fluorescence than the wild-type (A) and *Alas2*-null definitive erythroblasts (B). (D) Histogram of DCFHDA-mediated fluorescence: the wild-type definitive erythroblasts (filled curve); *Alas2*-null definitive erythroblasts (open curve). The open curve was shifted more to the right than the filled curve, suggesting that *Alas2*-null definitive erythroblasts are more peroxidized than the wild-type definitive erythroblasts.

It should be noted that ALAS1, the nonspecific form of  $\delta$ -aminolevulinic synthase, was up-regulated in *Alas2*-null definitive but down-regulated in the wild-type definitive erythroblasts, as compared with TER119<sup>+</sup> mature erythroblasts from bone marrow (Figure 4B). During erythroid differentiation of MEL cells, the level of ALAS1 mRNA has been shown to decline in synchrony with an increase in intracellular heme content, reflecting the well-known feedback repression of ALAS1 by heme.<sup>24</sup> Thus, both ALAS1 down-regulation in the wild-type definitive erythroblasts and its up-regulation in *Alas2*-null definitive erythroblasts appear to be under heme-mediated negative feedback control as in the liver and in MEL cells,<sup>25-27</sup> and the loss of the feedback repression by heme of ALAS1 in *Alas2*-null definitive erythroblasts may be a compensatory mechanism for their heme deficiency. However, mature erythroblasts must make an enormous amount of heme for hemoglobin formation, and limited contribution by ALAS1 would be insignificant.

Iron is known to produce reactive oxygen radicals that are highly toxic to cells.<sup>28</sup> It has been shown that ferritin iron, if accumulated in excess, can also participate in the generation of

reactive oxygen species and cause oxidative tissue damages.<sup>29,30</sup> In this study, we found that *Alas2*-null definitive erythroblasts were more capable of oxidation of a fluorogenic substrate, DCFHDA, than were the wild-type definitive erythroblasts. It is also known that erythrocytes in patients with sickle cell anemia and thalassemia contain excess amounts of iron and peroxidative lipids in the membrane.<sup>31</sup> Erythroid cells in patients with XLSA may also be more susceptible to oxidative damages than are normal erythroid cells, and such a mechanism may aggravate anemia. If this is the case, treatment of XLSA with iron-chelating agents and/or antioxidants might be of use and should merit clinical evaluation.

## Acknowledgments

The authors thank Ms C. Suzuki, Ms Y. Nishiyama, Ms K. Sato, Ms K. Kozawa, Ms A. Aizawa, Dr T. Miura, and Dr H. Ohtsu for their technical assistance. We are also grateful to Dr T. Nakano for providing OP9 cells and to Dr A. P. Doke for reviewing the manuscript.

## References

- Ponka P. Tissue-specific regulation of iron metabolism and heme synthesis: distinct control in erythroid cells. *Blood*. 1997;89:1-25.
- Chen JJ, London IM. Regulation of protein synthesis by heme-regulated eIF-2  $\alpha$  kinase [review]. *Trends Biochem Sci*. 1995;20:105-108.
- Muta K, Krantz SB. Inhibition of heme synthesis induces apoptosis in human erythroid progenitor cells. *J Cell Physiol*. 1995;163:38-50.
- Cox TC, Bawden MJ, Abraham NG, et al. Erythroid 5-aminolevulinic synthase is located in the X chromosome. *Am J Hum Genet*. 1990;46:107-111.
- Bottomley SS, May BK, Cox TC, Cotter PD, Bishop DF. Molecular defects of erythroid 5-aminolevulinic synthase in X-linked sideroblastic anemia. *J Bioenerg Biomembr*. 1995;27:161-168.
- Harigae H, Furuyama K, Kudo K, et al. A novel mutation of the erythroid-specific  $\delta$ -aminolevulinic synthase gene in a patient with non-inherited pyridoxine-responsive sideroblastic anemia. *Am J Hematol*. 1999;62:112-114.
- Harigae H, Furuyama K, Kimura A, et al. A novel mutation of the erythroid-specific  $\delta$ -aminolevulinic synthase gene in a patient with X-linked sideroblastic anemia. *Br J Haematol*. 1999;106:175-177.
- Riddle RD, Yamamoto M, Engel JD. Expression of  $\delta$ -aminolevulinic synthase in avian cells: separate genes encode erythroid-specific and nonspecific isozymes. *Proc Natl Acad Sci U S A*. 1989;86:792-796.
- Kappas A, Sassa S, Galbraith RA, Nordmann Y. The porphyria. In: Scriver CR, Beaudet AL, Sly WS, Valle D, eds. *The Metabolic and Molecular Basis of Inherited Disease*. Vol 7. New York, NY: McGraw-Hill; 1995:2103-2159.
- Nakajima O, Takahashi S, Harigae H, et al. Heme deficiency in the erythroid lineage causes differentiation arrest and cytoplasmic iron overload. *EMBO J*. 1999;18:6282-6289.
- Nakano T, Kodama H, Honjo T. In vitro development of primitive and definitive erythrocytes from different precursors. *Science*. 1996;272:722-724.
- Chomczynski P, Sacchi N. Single-step method of RNA isolation by acid guanidinium thiocyanate-phenol-chloroform extraction. *Anal Biochem*. 1987;162:156-159.
- Ikuta K, Kina T, MacNeil I, et al. A developmental switch in thymic lymphocyte maturation potential occurs at the level of hematopoietic stem cells. *Cell*. 1990;62:863-874.
- Sassa S. Sequential induction of heme pathway enzymes during erythroid differentiation of mouse Friend leukemia virus-infected cells. *J Exp Med*. 1976;143:305-315.
- Chan JY, Kwong M, Lo M, Emerson R, Kuypers FA. Reduced oxidative-stress response in red blood cells from p45NFE2-deficient mice. *Blood*. 2001;97:2151-2158.
- Nagai T, Harigae H, Ishihara H, et al. Transcription factor GATA-2 is expressed in erythroid, early myeloid, and CD34<sup>+</sup> human leukemia-derived cell lines. *Blood*. 1994;84:1074-1084.
- Miwa Y, Atsumi T, Imai N, Ikawa Y. Primitive erythropoiesis of mouse teratocarcinoma stem cells PCC3/A1 in serum-free medium. *Development*. 1991;111:543-549.
- Harigae H, Suwabe N, Weinstock PH, et al. Deficient heme and globin synthesis in embryonic stem cells lacking the erythroid-specific  $\delta$ -aminolevulinic synthase gene. *Blood*. 1998;91:798-805.
- Mitani K, Fujita H, Sassa S, Kappas A. Activation of heme oxygenase and heat shock protein 70 genes by stress in human hepatoma cells. *Biochem Biophys Res Commun*. 1990;166:1429-1434.
- Linpisarn S, Satoh K, Mikami T, Orimo H, Shinjo S, Yoshino Y. Effects of iron on lipid peroxidation. *Int J Hematol*. 1991;54:181-188.
- Fleming MD, Campagna DR, Haslett JN, Trenor CC III, Andrews NC. A mutation in a mitochondrial transmembrane protein is responsible for the pleiotropic hematological and skeletal phenotype of flexed-tail (*ft/ft*) mice. *Genes Dev*. 2001;15:652-657.
- Amenomori T, Tomonaga M, Jinnai I, et al. Cytogenetic and cytochemical studies on progenitor cells of primary acquired sideroblastic anemia (PASA): involvement of multipotent myeloid stem cells in PASA clone and mosaicism with normal clone. *Blood*. 1987;70:1367-1372.
- Takaku F, Mizoguchi H, Suda T, Kubota K, Miura Y. Erythroid precursor cells in primary acquired and secondary sideroblastic anemia. *Exp Hematol*. 1980;8:225-234.
- Fujita H, Yamamoto M, Yamagami T, Hayashi N, Sassa S. Erythroleukemia differentiation. Distinct responses of the erythroid-specific and the nonspecific  $\delta$ -aminolevulinic synthase mRNA. *J Biol Chem*. 1991;266:17494-17502.
- Sassa S, Granick S. Induction of  $\delta$ -aminolevulinic acid synthase in chick embryo liver cells in culture. *Proc Natl Acad Sci U S A*. 1970;67:517-522.
- Granick S, Sinclair P, Sassa S, Grieninger G. Effects by heme, insulin, and serum albumin on heme and protein synthesis in chick embryo liver cells cultured in a chemically defined medium, and a spectrofluorometric assay for porphyrin composition. *J Biol Chem*. 1975;250:9215-9225.
- Tyrell DL, Marks GS. Drug-induced porphyrin biosynthesis. Effect of protohemin on the transcriptional and post-transcriptional phases of  $\delta$ -aminolevulinic acid synthase induction. *Biochem Pharmacol*. 1972;21:2077-2093.
- Andrews NC. Disorders of iron metabolism. *N Engl J Med*. 1999;341:1986-1995.
- Gutteridge JM, Halliwell B, Treffry A, Harrison PM, Blake D. Effect of ferritin-containing fractions with different iron loading on lipid peroxidation. *Biochem J*. 1983;209:557-560.
- O'Connell MJ, Ward RJ, Baum H, Peters TJ. The role of iron in ferritin- and haemosiderin-mediated lipid peroxidation in liposomes. *Biochem J*. 1985;229:135-139.
- Shalev O, Repka T, Goldfarb A, et al. Deferiprone (L1) chelates pathologic iron deposits from membranes of intact thalassemic and sickle red blood cells both in vitro and in vivo. *Blood*. 1995;86:2008-2013.